

PAPER • OPEN ACCESS

Magnetotransport phenomena and spin accumulation in MIS structures

To cite this article: N V Volkov *et al* 2019 *J. Phys.: Conf. Ser.* **1347** 012006

View the [article online](#) for updates and enhancements.



IOP | ebooks™

Bringing together innovative digital publishing with leading authors from the global scientific community.

Start exploring the collection—download the first chapter of every title for free.

Magnetotransport phenomena and spin accumulation in MIS structures

N V Volkov¹, I A Bondarev^{1,2}, A S Tarasov¹, M V Rautskii¹, A V Lukyanenko^{1,2},
D A Smolyakov¹, S N Varnakov¹ and S G Ovchinnikov¹

¹ Kirensky Institute of physics of the Krasnoyarsk Scientific Center of the Siberian Branch of the Russian Academy of Sciences, 660036, Krasnoyarsk, Russia

² Institute of engineering physics and radio electronics, Siberian Federal University, 660041, Krasnoyarsk, Russia

Abstract. The present work is devoted to magnetic transport in Fe/SiO₂/p-Si, Mn/SiO₂/p-Si and Fe₃Si/p-Si hybrid structure. For Mn/SiO₂/p-Si diode extremely large values of magnetoresistance were observed (10⁵ % for AC and 10⁷ % for DC) which is explained by impact ionization process that can be suppressed by the magnetic field. Lateral photovoltaic effect in Fe/SiO₂/p-Si have also shown a strong dependence on the magnetic field in low-temperature region (the relative change of photovoltage exceeded 10³ %). In Fe₃Si/p-Si spin accumulation was found via 3-terminal Hanle measurements. We believe that the magnetic field affects electric transport through Lorentz force and through the interface states which are localized at the insulator/semiconductor or metal/semiconductor interfaces. Such states play a decisive role in magnetotransport as their energy can be controlled by a magnetic field. In Fe₃Si/p-Si they also participate in spin-dependent tunneling, causing spin injection from the Fe₃Si film into the silicon.

1. Introduction

Structures with ferromagnetic layers have been intensively studied since the discovery of the giant magnetoresistance effect [1]. Later, the interest in ferromagnetic metal/insulator/semiconductor (MIS) hybrid structures had arisen [2]. Compatibility with CMOS and SOI technology as well as the possibility to induce and control the spin-dependent transport allowed MIS structures to find practical applications in different magnetic and spintronic devices such as magnetic field sensors, memory and logic devices [3-6]. Recent advances in the study of hybrid structures may lay in a basis of the future spin transistor.

Our investigations of the AC and DC magnetic transport in MIS structures revealed the unusual effects, which are not directly spin-dependent. We observed the AC and DC giant magnetoresistance in Fe/SiO₂/p-Si and Mn/SiO₂/p-Si diodes with the Schottky barrier [7-10]. The assumption was made that one of the mechanisms of the MR effects in our structures is related to surface states localized at the insulator/semiconductor interface. These states are involved in the recharging process and can be affected by magnetic field.

In order to study the interplay between the electricity, magnetism and optical irradiation in our structures we measured the lateral photovoltaic effect (LPE). LPE was discovered by Schottky [11] and Wallmark [12] and found its application in position detectors due to the high sensitivity to a laser



spot position [13]. Photovoltaic effect in $\text{Fe}/\text{SiO}_2/\text{p-Si}$ showed surprisingly high sensitivity to a magnetic field.

One of the most interesting results obtained is the spin accumulation in low doped silicon in the epitaxial $\text{Fe}_3\text{Si}/\text{p-Si}$ structure [14]. Similar results had been reported in [15-17], however the spin accumulation was observed either in structures with insulating barrier, or in structures with highly doped substrates ($6 \cdot 10^{19} \text{ cm}^{-3}$) compared to our case ($2 \cdot 10^{15} \text{ cm}^{-3}$). Main conclusion is that detected localized interface states are involved in all observed magneto- and spin-dependent effects.

2. Materials and methods

In present work we will consider $\text{Me}/\text{SiO}_2/\text{p-Si}$ (where Me are Fe and Mn) and $\text{Fe}_3\text{Si}/\text{p-Si}$ structures. Detailed description of sample fabrication can be found in [18-20] for $\text{Me}/\text{SiO}_2/\text{Si}$ and in [14] for $\text{Fe}_3\text{Si}/\text{p-Si}$. Samples were fabricated on boron doped Si substrates. All films were deposited by thermal evaporation at ultrahigh vacuum conditions in Angara chamber [21] providing polycrystalline and epitaxial growth. Before film deposition in $\text{Me}/\text{SiO}_2/\text{p-Si}$, SiO_2 layer was formed by exposing in aqueous solution of H_2O_2 and NH_4OH . In case of $\text{Fe}_3\text{Si}/\text{p-Si}$ structure oxide was removed by high temperature annealing at vacuum chamber. Parameters of the samples are presented in Table 1.

Table 1. Parameters of the $\text{Me}/\text{SiO}_2/\text{p-Si}$ and $\text{Fe}_3\text{Si}/\text{p-Si}$ structures

	Substrate resistivity	Substrate orientation	Doping density N_A	Oxide thickness	Film thicknesses
$\text{Me}/\text{SiO}_2/\text{p-Si}$	$5 \Omega \text{ cm}$	(100)	$2 \cdot 10^{15} \text{ cm}^{-3}$	1.5 nm	10 nm
$\text{Fe}_3\text{Si}/\text{p-Si}$	$7.5 \Omega \cdot \text{cm}$	(111)		N/A	21 nm

The measurements were performed using different experimental schemes (figure 1). In order to study AC and DC electric transport, $\text{Me}/\text{SiO}_2/\text{p-Si}$ MIS Shottky diodes were fabricated (figure 1a). Indium ohmic contacts were attached to the substrate backside. Lateral device for measuring LPE is shown on figure 1b. The sample was irradiated by a laser diode with $\lambda = 1 \mu\text{m}$. The light was focused into a narrow strip of 0.5 mm in width on the structure surface. Spin accumulation in $\text{Fe}_3\text{Si}/\text{p-Si}$ was measured using 3-terminal planar microstructure (figure 1c) fabricated by conventional photolithography and wet chemical etching [22]. To perform electrical transport measurements samples were placed to helium cryostat with quartz window that is a part of a home-built facility [22] equipped with an electromagnet, Keithley 2634b SourceMeter, Keithley 2182a nanovoltmeter and Agilent E4980A LCR-meter. During the experiments, temperature varied from 4.2 K to 300 K and magnetic field swept up to 1 T.

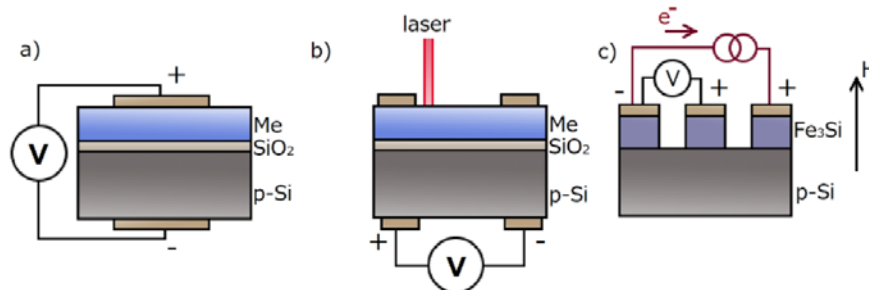


Figure 1. Experimental schemes: *a* — Schottky diode for AC and DC transport measurements; *b* — lateral device for measuring lateral photovoltaic effect; *c* — 3-terminal device for measuring spin accumulation.

3. Results

3.1. Magnetoresistance

Firstly, we will consider AC transport in Mn/SiO₂/p-Si structure [18,19]. Figure 2 shows magnetic field dependence of R_{ac} (the real part of the impedance) at $V_b = 0$ and 5 V where V_b is the bias voltage. At zero bias, we observe a giant magnetoresistance effect of about 200% which is typical for MIS structures. However, applying the forward bias drastically change $R_{ac}(H)$ behavior, and magnetoresistance (MR) value reaches 10⁵ %. The results obtained at reverse bias are similar to those for Fe/SiO₂/p-Si which are presented in [8-10].

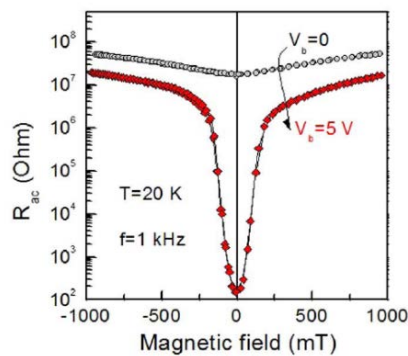


Figure 2. Field dependences of R_{ac} of the Mn/SiO₂/p-Si at $V_b = 0$ and 5 V, $T = 20$ K and $f = 1$ kHz.

DC resistance shows similar behavior, which can be seen from its temperature dependence (figure 3a) at $V_b = 3.5$ V. The MR value is even higher than for ac, and reaches the value of 10⁷ % (figure 3b). It can be seen from both ac and dc measurements, that the sharpest increase of MR appears in relatively low magnetic fields ($H < 250$ mT) at low temperatures below 40 K.

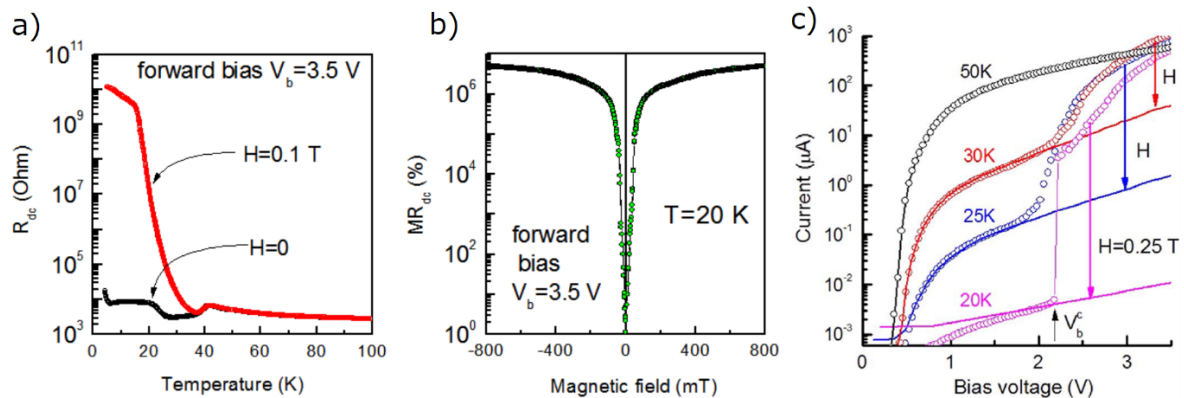


Figure 3. Temperature dependence of R_{dc} of the Mn/SiO₂/p-Si at $V_b = 3.5$ V, at $H = 0$ and 0.1 T (a) and MR_{dc} as a function of magnetic field at $T = 20$ K (b); c — I - V curves at $H = 0$ (open circles) and $H = 250$ mT (solid lines) at different temperatures.

The form of I - V characteristics has typical form for MIS Schottky diode (figure 3c) above 40 K. In low temperature region, current increases drastically when certain threshold V_b is applied. This means that the process of impact ionization takes place, which will be described in the discussion section. Magnetic field suppresses impact ionization as can be seen from the figure 3c. It explains the extremely large MR values in this temperature region.

3.2. Lateral photovoltaic effect

Lateral photovoltage in Fe/SiO₂/p-Si showed high sensitivity to a magnetic field [18,19]. Figure 4 shows temperature dependences of lateral photovoltage measured from the substrate as shown in

figure 1b at different values of H . We defined a relative change of photovoltage in a magnetic field as $MV = (PV(H) - PV(0))/PV(0)$. At $T > 30$ K the value of MV does not exceed 10-20%. However, at $T < 30$ K much more complicated magnetic field dependence of LPV is observed. Below 30 K PV decreases and changes sign near 12 K. The highest MV is observed below 10 K and can exceed 10^3 % in a field of 700 mT.

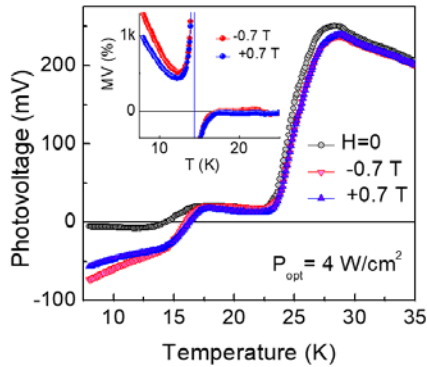


Figure 4. LPV as function of temperature at $H = 0$, 0.7 T, -0.7 T and $P = 4$ W/cm². Inset: MV as function of temperature at positive and negative fields.

3.3. Spin accumulation

In order to study the spin-dependent transport, we used the epitaxial Fe₃Si/*p*-Si structure as a sample [14]. Firstly, we checked the necessary electrical properties such as film resistivity and Schottky barrier parameters. Fe₃Si shows metallic type of conductivity from 4 to 300 K. The resistivity values in this temperature region vary from 55 μOhm·cm to 120 μOhm·cm which is typical for Fe₃Si films [23,24]. Parameters of the Schottky barrier were extracted from the I - V characteristic of the prepared diode (figure 5). Ohmic contact on substrate backside was made by indium alloying (right inset on figure 5). The diode shows typical rectifying behavior. By analyzing the direct branch of the I - V curve via Cheung's method [25], we calculated the barrier height which is $\phi_{Bp} = 0.57$ eV. It is an adequate value for M/S diode based on *p*-Si substrate and can provide spin injection from Fe₃Si to *p*-Si.

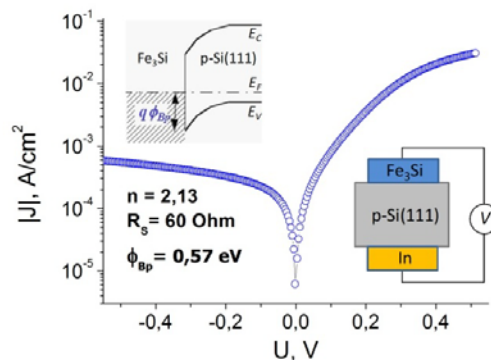


Figure 5. I - V characteristic of the Fe₃Si/*p*-Si diode at $T = 295$ K. The right and left insets show schematic illustrations of the experimental scheme for Fe₃Si/Si(111) diode and an energy diagram of the Schottky barrier for Fe₃Si/*p*-Si(111) structure respectively

Measurements of the spin accumulation were performed by three-terminal Hanle technique [26]. The experimental scheme is shown on figure 1c. If the spin injection into a semiconductor is realized, then the external magnetic field perpendicular to a sample plane will cause spin precession and the spin accumulation will be reduced as it distributes deep into the semiconductor. As a result, $\Delta\mu(H)$ curve will have the Lorentzian shape. According to [2,27,28] accumulation is correlated with 3-terminal voltage signal as $\Delta V = A_{sp}\Delta\mu/2$, where A_{sp} is efficiency coefficient of spin injection from ferromagnetic metal into semiconductor.

$\Delta V(H_z)$ curves for our structure are presented in figure 6 where ΔV is 3-terminal voltage signal and H_z is magnetic field oriented perpendicular to the sample plane. Experimental results are in good agreement with Lorentz fitted curves (solid lines) which indicates spin accumulation in silicon.

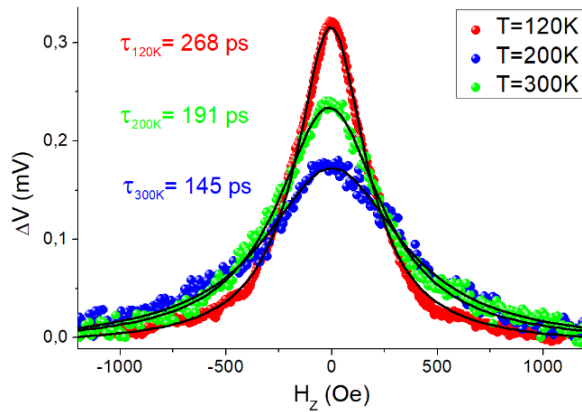


Figure 6. Experimental Hanle curves of the $\text{Fe}_3\text{Si}/p\text{-Si}$ structure at $T = 120, 200$ and 300 K (circles) and Lorentzian fits (solid lines).

By the analysis of Lorentzian curve, spin lifetime values were calculated from the expression $\tau_s = 1/\omega_L = h/2\pi g_h \mu_B \Delta B$ where ΔB is half-width of the curve in its half-max, g_h is Lande g -factor of holes ($g_h = 2$). The calculated values are $\tau_{300\text{K}} = 145$ ps, $\tau_{200\text{K}} = 191$ ps and $\tau_{120\text{K}} = 268$ ps. These are typical for silicon.

It is interesting that the spin injection is realized in $\text{Fe}_3\text{Si}/p\text{-Si}$ despite the absence of an insulating tunnel barrier or narrow Schottky barrier contact, like in other works [15,17]. We believe that the spin dependent tunneling is realized through the interface states which will be discussed in the next section.

4. Discussion

In the following section we will discuss the possible mechanisms of the magnetic field effect on the transport properties as well as the role, played by the interface states. As was shown in figure 3c, the I - V curves of the MIS diode below 50 K demonstrate the rapid increase of current when the bias voltage exceeds certain threshold value. It is caused by the shallow acceptor boron states in the bulk of the semiconductor. When the high enough bias voltage is applied, carriers acquire the kinetic energies which exceed the ionization energy of acceptor impurities. It leads to the autocatalytic process of impact ionization [29]. Magnetic field affects impact ionization process via two mechanisms. Firstly, it increases the energy of acceptor levels [8], therefore higher kinetic energy is required to initiate impact ionization and the threshold voltage increases. The second mechanism is Lorentz force. It deflects carriers' trajectories, increasing the probability of inelastic scattering and decreasing kinetic energy, suppressing impact ionization. In order to restore it, the higher bias voltage is required, which also leads to the increase of the threshold voltage.

The same mechanisms are responsible for the magnetic field influence on LPE (figure 4). At $T > 27$ K, Lorentz force deflects trajectories of photoinduced carriers which drift in lateral direction under the action of the space-charge region field $\varepsilon(z)$. It increases the recombination probability and the decrease of LPV is observed. At $T < 27$ K, magnetic field increases the energies of acceptor states E_a including the surface states which are localized at the SiO_2/Si interface. E_a levels become higher than the Fermi level for an increasing number of interface states, resulting in the decreasing of acceptor density and consequently decreasing of $\varepsilon(z)$. The relative contribution of the electrons diffusion into the semiconductor increases and the LPV caused by nonequilibrium carriers increases.

As for the spin-dependent transport in the $\text{Fe}_3\text{Si}/p\text{-Si}$ structure, magnetic field decreases spin accumulation inside the semiconductor via Hanle effect. Considering the fact that our structure doesn't have an insulating tunnel barrier or narrow Schottky barrier contact, we believe that the spin injection is realized by the spin-dependent tunneling through interface states [30]. It is confirmed by the fact that the efficiency of the spin-dependent tunneling depends weakly on temperature and changing the carriers' mobility can increase spin lifetime only by 30-50% [30]. And in our case, it can be increased almost twice (figure 6) [31,32].

5. Conclusion

In summary, it is clear that the decisive role in magnetotransport and spin-dependent effects is played by the interface states, which energy can be controlled by a magnetic field in order to manipulate the electric transport. Such states can be also used to replace insulating barriers or Shottky contacts and provide the spin dependent tunneling into a semiconductor.

Acknowledgements

The reported study was funded by Russian Foundation for Basic Research, project No 17-02-00302.

References

- [1] Baibich M N, Broto J M, Fert A, Van Dau F N, Petroff F, Etienne P and Chazelas J 1988 *Phys. Rev. Lett.* **61**(21) 2472
- [2] Fert A and Jaffres H 2001 *Phys. Rev. B* **64**(18) 184420
- [3] Žutić I, Fabian J and Sarma S D 2004 *Rev. Modern Phys.* **76**(2) 323
- [4] Joo S, Kim T, Shin S H, Lim J Y, Hong J, Song J D and Shin K H 2013 *Nature* **494**(7435) 72
- [5] Kiselev S I, Sankey J C, Krivorotov I N, Emley N C, Schoelkopf R J, Buhrman R A and Ralph D C 2003 *Nature* **425**(6956) 380
- [6] Suzuki Y and Kubota H 2008 *J. Phys. Soc. Jap.* **77**(3) 031002
- [7] Volkov N V, Tarasov A S, Eremin E V, Varnakov S N, Ovchinnikov S G and Zharkov S M 2011 *J. Appl. Phys.* **109**(12) 123924
- [8] Volkov N V, Tarasov A S, Eremin E V, Eremin A V, Varnakov S N and Ovchinnikov S G 2012 *J. Appl. Phys.* **112**(12) 123906
- [9] Volkov N V, Tarasov A S, Eremin E V, Baron F A, Varnakov S N and Ovchinnikov S G 2013 *J. Appl. Phys.* **114**(9) 093903
- [10] Volkov N V, Tarasov A S, Smolyakov D A, Gustaitsev A O, Balashev V V and Korobtsov V V 2014 *Appl. Phys. Lett.* **104**(22) 222406
- [11] Schottky W 1930 *Phys. Z.* **31** 913
- [12] Wallmark J T 1957 *Proc. IRE* **45**(4) 474
- [13] Pereira L, Costa D, Fortunato E and Martins R 2005 *J. Mater. Sci.* **40**(6) 1377
- [14] Tarasov A S, Bondarev I A, Rautskii M V, Lukyanenko A V, Tarasov I A, Varnakov S N and Volkov N V 2018 *J. Surf. Investigat. X-ray Synchr. Neutron Techniq.* **12**(4) 633
- [15] Spiesser A, Sharma S, Saito H, Jansen R, Yuasa S and Ando K 2012 *Proc. SPIE Spintronics V ed H-J Drouhin, J-E Wegrowe, M Razeghi* **8461** 84610K
- [16] Dash S P, Sharma S, Le Breton J C, Peiro J, Jaffrès H, George J M and Jansen R 2011 *Phys. Rev. B* **84**(5) 054410
- [17] Fujita Y, Yamada S, Ando Y, Sawano K, Itoh H, Miyao M and Hamaya K 2013 *J. Appl. Phys.* **113**(1) 013916
- [18] Volkov N V, Tarasov A S, Rautskii M V, Lukyanenko A V, Bondarev I A, Varnakov S N and Ovchinnikov S G 2018 *J. Magnet. Magnetic Mater.* **451** 143
- [19] Volkov N V, Rautskii M V, Tarasov A S, Yakovlev I A, Bondarev I A, Lukyanenko A V and Ovchinnikov S G 2018 *Phys. E* **101** 201
- [20] Volkov N V, Tarasov A S, Smolyakov D A, Gustaitsev A O, Rautskii M V, Lukyanenko A V and Ovchinnikov S G 2017 *AIP Advances*, **7**(1) 015206
- [21] Varnakov S N, Lapeshev A A, Ovchinnikov S G, Parshin A S, Korshunov M M and Nevorol P 2004 *Instrum. Experim. Techniq.* **47**(6) 839
- [22] Tarasov A S, Lukyanenko A V, Rautskii M V, Bondarev I A, Smolyakov D A, Tarasov I A and Volkov N V 2019 *Semicond. Sci. Technol.* **34**(3) 035024
- [23] Vinzelberg H, Schumann J, Elefant D, Arushanov E and Schmidt O G 2008 *J. Appl. Phys.* **104**(9) 093707
- [24] Hung H Y, Huang S Y, Chang P, Lin W C, Liu Y C, Lee S F and Kwo J 2011 *J. Cryst. Growth* **323**(1) 372

- [25] Cheung S K and Cheung N W 1986 *Appl. Phys. Lett.* **49**(2) 85
- [26] Jansen R, Dash S P, Sharma S and Min B C 2012 *Semicond. Sci. Technol.* **27**(8) 083001
- [27] Osipov V V and Bratkovsky A M 2005 *Phys. Rev. B* **72**(11) 115322
- [28] Dash S P, Sharma S, Patel R S, de Jong M P and Jansen R 2009 *Nature* **462**(7272) 491
- [29] Cohen M E and Landsberg P T 1967 *Phys. Rev.* **154**(3) 683
- [30] Dankert A, Dulal R S and Dash S P 2013 *Sci. Reports* **3** 3196
- [31] Tran M, Jaffrès H, Deranlot C, George J M, Fert A, Miard A and Lemaître A 2009 *Phys. Rev. Lett.* **102**(3) 036601
- [32] Jansen R, Deac A M, Saito H and Yuasa S 2012 *Phys. Rev. B* **85**(13) 134420